

Discovery potential for charmonium-like state $Y(3940)$ by the meson photoproduction

Jun He^{1,2*} and Xiang Liu^{1,3†‡}

¹*Research Center for Hadron and CSR Physics, Lanzhou University
& Institute of Modern Physics of CAS, Lanzhou 730000, China*

²*Institute of Modern Physics, Chinese Academy of Sciences, Lanzhou 730000, China*

³*School of Physical Science and Technology, Lanzhou University, Lanzhou 730000, China*

(Dated: February 4, 2022)

In this work, we investigate the discovery potential for $Y(3940)$ by the photoproduction process $\gamma p \rightarrow Y(3940)p$. The numerical result shows that the upper (lower) limit of the total cross section for $\gamma p \rightarrow Y(3940)p$ is up to the order of 1 nb (0.1 μ b). Additionally, the background analysis and the Dalitz plot relevant to the production of $Y(3940)$ are studied. The Dalitz plot analysis of $Y(3940)$ production indicates that $Y(3940)$ signal can be distinguished from the background clearly. The lower limit of the number of events of $Y(3940)$ reaches up to 10/0.02GeV² for 1×10^9 collisions of γp by studying the invariant mass spectrum of $J/\psi\omega$. An experimental search for $Y(3940)$ by the meson photoproduction is suggested.

PACS numbers: 14.40.Lb, 13.60.Le, 12.39.Fe

I. INTRODUCTION

With the development of the experimental technology, experiments have announced a series of charmonium-like states X , Y , Z in the past six years. Among these charmonium-like states, $Y(3940)$ is an enhancement near the threshold of $J/\psi\omega$ in exclusive $B \rightarrow K\omega J/\psi$ decay [1, 2]. The experimental information given by the Belle and Babar Collaborations is summarized in Table I. Although the values of mass and width given by the Babar Collaboration are

| Experiment | Mass (MeV) | Width (MeV) | $\mathcal{B}[B \rightarrow KY(3940)]\mathcal{B}[Y(3940) \rightarrow J/\psi\omega]$ |
|------------|--------------------------------------------------------|-------------------------------------------------|------------------------------------------------------------------------------------|
| Belle [1] | $3943 \pm 11(\text{stat}) \pm 13(\text{syst})$ | $87 \pm 22(\text{stat}) \pm 26(\text{syst})$ | $(7.1 \pm 1.3(\text{stat}) \pm 3.1(\text{syst})) \times 10^{-5}$ |
| Babar [2] | $3914^{+3.8}_{-3.4}(\text{stat}) \pm 2.0(\text{syst})$ | $34^{+12}_{-8}(\text{stat}) \pm 5(\text{syst})$ | $(4.9^{+1.0}_{-0.9}(\text{stat}) \pm 0.5(\text{syst})) \times 10^{-5}$ |

TABLE I: The mass, width and product branching fraction of $Y(3940)$ measured by the Belle and Babar experiments.

smaller than those reported by the Belle Collaboration, the measured product branching ratios by Belle and Babar agree with each other. As indicated in Refs. [3, 4], taking the typical value for allowed $B \rightarrow K + \text{charmonium}$ decays ($\mathcal{B}[B \rightarrow KY(3940)] \leq 1 \times 10^{-3}$), one obtains the lower limit of the decay width of $Y(3940) \rightarrow J/\psi\omega$, which means $\Gamma[Y(3940) \rightarrow J/\psi\omega] \geq 1$ MeV and $\Gamma[Y(3940) \rightarrow J/\psi\omega] \geq 4$ MeV corresponding to Babar and Belle results, respectively. Thus, to some extent, explaining $Y(3940)$ as a conventional charmonium state is problematic due to the unusual decay width of $Y(3940) \rightarrow J/\psi\omega$ [4].

In the past years, theorists have been puzzled with the underlying structure of $Y(3940)$ after the observation of $Y(3940)$. With the observation of $Y(4140)$ by the CDF [5], the similarities between $Y(4140)$ and $Y(3940)$ provide the hint to reveal the structure of $Y(3940)$. Thus, the explanations of $D^*\bar{D}^*$ and $D_s^*\bar{D}_s^*$ respectively corresponding to $Y(3940)$ and $Y(4140)$ were proposed in Refs. [6, 7]. The possible quantum number assignment includes $J^{PC} = 0^{++}$ or $J^{PC} = 2^{++}$ [6].

It is well-known that most of charmonium-like states are only observed in the two B factories by B meson decay, which provides the $c\bar{c}$ rich environment. However, searching for X , Y , Z charmonium-like states by other production processes is an interesting topic, which will not only confirm these observed charmonium-like states, but also be helpful to study their underlying structures. For example, theorists carried out the relevant studies of the production of $Z^\pm(4430)$, which is an enhancement in the $\psi'\pi^\pm$ invariant mass spectrum [8]. Liu, Zhao, and Close once proposed to search for $Z^\pm(4430)$ by the meson photoproduction process [9]. Additionally, the authors in Ref. [10] suggested an experiment to find the signal of $Z^\pm(4430)$ by the nucleon-antinucleon scattering.

[†] Corresponding author

^{*}Electronic address: junhe@impcas.ac.cn

[‡]Electronic address: xiangliu@lzu.edu.cn

Meson photoproduction is an important way to study hadron spectroscopy, such as the baryon resonances and charmonium with a higher beam energy [11, 12, 13]. The thresholds for X, Y, Z photoproductions fall in the energy region of the HERA experiment. Thus, it is interesting to study whether there exists a potential to find $Y(3940)$ by meson photoproduction. In this work we will be dedicated to exploring $Y(3940)$ production by the photoproduction process.

The paper is organized as follows. After the introduction, we present the calculation of $Y(3940)$ photoproduction. In Sec. III, the possible background relevant to the production of $Y(3940)$ is discussed and the Dalitz plot is presented. The last section is the conclusion and discussion.

II. $Y(3940)$ IN THE PHOTOPRODUCTION PROCESS

In this section, we will discuss the production probability of $Y(3940)$ through calculating the cross section of the photoproduction process. As shown in the introduction, Babar and Belle reported the observation of $Y(3940)$ in the decay channel to J/ψ and ω . Since both J/ψ and ω interact with a photon via the well-known vector meson dominance mechanism, the $Y(3940)$ photoproduction process can be described by Fig. 1. Here, the t channel is the dominant process due to the threshold of $Y(3940)$ photoproduction being about 4 GeV.

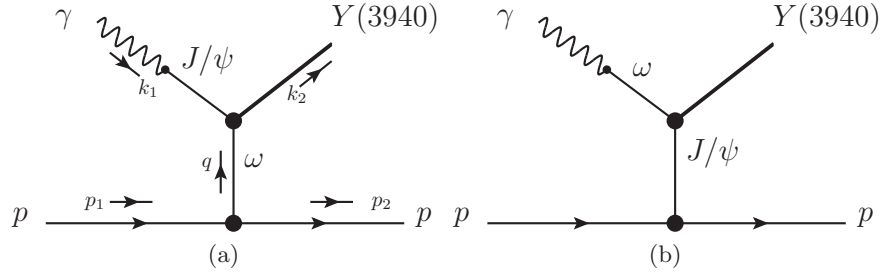


FIG. 1: The $Y(3940)$ photoproductions through ω and J/ψ exchanges.

Considering the coupling between J/ψ and the nucleon being obviously weaker than that between ω and the nucleon, in this work one mainly discusses the photoproduction process depicted in Fig. 1 (a). Here, the ω meson is the exchanged state and J/ψ is as the intermediate vector meson coupling to the incoming photon. Since the contribution from the pomeron exchange is negligible as discussed in Ref. [9], we do not consider the contribution of the pomeron exchange to the $Y(3940)$ photoproduction process in this work.

As discussed in Ref. [6], the charmonium-like state $Y(3940)$ may have a quantum number $J^{PC} = 0^{++}$ or 2^{++} . The vertices depicting the interaction of $Y(3940)$ and $J/\psi\omega$ are [14, 15, 16, 17]

$$\langle J/\psi(k_1)\omega(k_2)|Y(3940)\rangle = \frac{g_{YJ/\psi\omega}}{M_Y}\epsilon_1^\mu\epsilon_2^\nu T_{\mu\nu}, \quad \text{for } 0^{++} \quad (1)$$

$$\langle J/\psi(k_1)\omega(k_2)|Y(3940)\rangle = \frac{g_{YJ/\psi\omega}}{M_Y}\epsilon_1^\mu\epsilon_2^\nu\epsilon^{\alpha\beta}M_{\mu\nu,\alpha\beta}, \quad \text{for } 2^{++} \quad (2)$$

with

$$T_{k_1,k_2}^{\mu\nu} = g^{\mu\nu}k_1 \cdot k_2 - k_1^\nu k_2^\mu, \quad (3)$$

$$M_{k_1,k_2}^{\mu\nu,\alpha\beta} = g^{\nu\beta}k_1^\alpha k_2^\mu + g^{\mu\alpha}k_1^\nu k_2^\beta - g^{\mu\nu}k_1^\alpha k_2^\beta - g^{\mu\alpha}g^{\nu\beta}k_1 \cdot k_2, \quad (4)$$

where ϵ^μ and $\epsilon^{\mu\nu}$ are the polarization vector and the polarization tensor corresponding to $Y(3940)$ with $J^P = 0^{++}$ and $J^P = 2^{++}$, respectively. The Lagrangians listed in Eqs. (1) and (2) are derived using gauge invariance and vector and tensor meson dominance. We adopt the lower (upper) limit of the decay width of $Y(3940) \rightarrow J/\psi\omega$, $\Gamma[Y(3940) \rightarrow J/\psi\omega] = 1(34)$ MeV [2, 3, 4], to determine the lower (upper) limit of the coupling constant: $g_{YJ/\psi\omega} = 0.264(1.54)$ GeV^{-1} for scalar $Y(3940)$ or $g_{YJ/\psi\omega} = 0.461(2.69)$ GeV^{-1} for tensor $Y(3940)$. Additionally, for describing the vertex with the off-shell ω , we introduce the monopole form factor $F_{YJ/\psi\omega}(q^2) = (\Lambda_Y^2 - m_\omega^2)/(\Lambda_Y^2 - q^2)$, where we set the cutoff Λ_Y as the mass of J/ψ as suggested in Ref. [9].

In the vector meson dominance mechanism, the Lagrangian depicting the coupling of the intermediate state J/ψ with photon is written as

$$\mathcal{L}_{J/\psi\gamma} = -\frac{eM_{J/\psi}^2}{f_{J/\psi}}V_\mu A^\mu, \quad (5)$$

where $M_{J/\psi}$ and $f_{J/\psi}$ denote the mass and the decay constant of J/ψ respectively. In terms of the decay width of $J/\psi \rightarrow e^+e^-$ [18]

$$\Gamma_{J/\psi \rightarrow e^+e^-} = 5.55 \pm 0.14 \pm 0.02 \text{ keV},$$

one obtains the parameter $e/f_{J/\psi} = 0.027$.

We adopt the effective Lagrangian

$$\mathcal{L}_{\omega NN} = -g_{\omega NN}\bar{N}(\gamma \cdot \omega - \frac{\kappa_\omega}{2M_N}\sigma^{\mu\nu}\partial_\nu\omega_\mu)N \quad (6)$$

to describe the coupling between ω and the nucleon. Besides, one introduces the monopole form factor $F_{\omega NN} = (\Lambda_\omega^2 - m_\omega^2)/(\Lambda_\omega^2 - q^2)$ in $NN\omega$ vertex to compensate the off-shell effect of the ω meson. Here, $g_{\omega NN} = 12$, $\kappa_\omega = 0$ and $\Lambda_\omega = 1.2 \text{ GeV}$ [19]. The vertex of $J/\psi\omega Y$ is result of the vector meson dominance mechanism. Thus, there exists the difference of the vertex of $NN\omega$ from the vertex of $J/\psi\omega Y$. We distinguish the vertex of $NN\omega$ and the vertex of $J/\psi\omega Y$ by introducing different cutoff Λ_Y and Λ_ω corresponding to the vertex of $NN\omega$ and the vertex of $J/\psi\omega Y$ respectively.

The differential cross section for $Y(3940)$ photoproduction shown in Fig. 1 (a) reads as

$$\frac{d\sigma}{dt} = \frac{1}{256\pi s} \frac{1}{|k_{1cm}|^2} \sum_{pol} |\mathcal{T}_{fi}|^2, \quad (7)$$

where $s = (p_1 + k_1)^2 = (p_2 + k_2)^2 = W^2$ and $t = (k_2 - k_1)^2 = (p_1 - p_2)^2 = q^2$ denote the Mandelstam variables. k_{1cm} is the photon energy in the center of mass frame of γp scattering.

The amplitude \mathcal{T}_{fi} for the production of scalar $Y(3940)$ is obtained

$$\mathcal{T}_{fi} = \left(g_{\omega NN} \frac{g_{YJ/\psi\omega}}{M_Y} \frac{e}{f_{J/\psi}}\right) \bar{u}(p_2) O^\alpha u(p_1) \epsilon_{1\alpha}, \quad (8)$$

where

$$O^\alpha = G^\mu \frac{\bar{g}_{\mu\nu}}{q^2 - m_\omega^2} A^{\nu\alpha}, \quad G^\mu = \gamma^\mu F_{\omega NN}(q^2), \quad A^{\nu\alpha} = T_{k_1, q_1}^{\alpha\nu} F_{YJ/\psi\omega}(q^2).$$

Analogously, for the $\gamma p \rightarrow Y(3940)p$ with tensor $Y(3940)$, the amplitude \mathcal{T}_{fi} is

$$\mathcal{T}_{fi} = \left(g_{\omega NN} \frac{g_{YJ/\psi\omega}}{M_Y} \frac{e}{f_{J/\psi}}\right) \bar{u}(p_2) O^{\alpha, \beta\gamma} u(p_1) \epsilon_{1\alpha} \epsilon_{\beta\gamma}, \quad (9)$$

with

$$O^{\alpha, \beta\gamma} = G^\mu \frac{\bar{g}_{\mu\nu}}{q^2 - m_\omega^2} A^{\nu\alpha, \beta\gamma}, \quad G^\mu = \gamma^\mu F_{\omega NN}(q^2), \quad A^{\nu\alpha, \beta\gamma} = M_{k_1, q_1}^{\alpha\nu, \beta\gamma} F_{YJ/\psi\omega}(q^2).$$

In the above expressions, we define $\bar{g}_{\mu\nu} = -g_{\mu\nu} + q_\mu q_\nu / m_\omega^2$. Since, the longitudinal part of the omega-meson propagator does not contribute to the amplitudes, we use $\bar{g}_{\mu\nu} = -g_{\mu\nu}$ instead of $\bar{g}_{\mu\nu} = -g_{\mu\nu} + q_\mu q_\nu / m_\omega^2$ for writing out the amplitude.

With the above preparation, we obtain the differential cross section for $Y(3940)$ production, which is shown in Fig. 2. After integrating over the range of t , the total cross section $\sigma(\gamma p \rightarrow Y(3940)p)$ is presented in Fig. 2.

These results show that a peak appears at the low $-q^2$ region. The line shape of the total cross section goes up very rapidly near the threshold, while the line shape of the differential cross section becomes flat with the increase of $-q^2$. The total cross section for the production of tensor $Y(3940)$ is about 5 times larger than that for the production of the scalar $Y(3940)$. The total cross section is proportional to the square of the coupling $g_{YJ/\psi\omega}$, which indicates

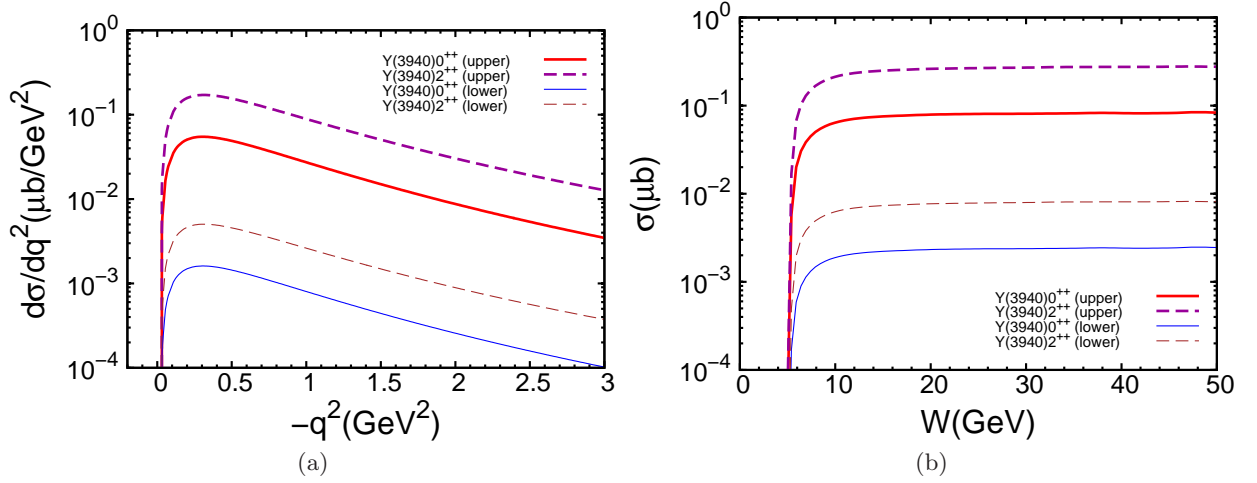


FIG. 2: The upper and lower limits of the cross sections for the production of $Y(3940)$ with quantum number 0^{++} or 2^{++} . (a) The variation of the differential cross sections of $\gamma p \rightarrow Y(3940)p$ to $-q^2$. (b) The dependence of the total cross section of $\gamma p \rightarrow Y(3940)p$ on the total energy in the center of mass frame of γp scattering.

that the cross section is also proportional to the decay width of $Y(3940) \rightarrow J/\psi\omega$. Since the concrete value of the decay width of $Y(3940) \rightarrow J/\psi\omega$ is undetermined by theory and experiment, we only give the upper and lower limits of $\sigma(\gamma p \rightarrow Y(3940)p)$ in this work according to the upper and lower limits of the decay width of $Y(3940) \rightarrow J/\psi\omega$. The upper limit of $\sigma(\gamma p \rightarrow Y(3940)p)$ under the two assignments of the quantum number for $Y(3930)$ is on the order of $0.1 \mu\text{b}$, which is comparable with the cross section of J/ψ photoproduction in the HERA experiment [11, 13]. The lower limit of $\sigma(\gamma p \rightarrow Y(3940)p)$ is a few nb , which is comparable with the cross section of $\psi(2S)$ [12] or bottomonium Υ photoproduction in HERA [20, 21].

III. BACKGROUND ANALYSIS AND DALITZ PLOT

Since the produced $Y(3930)$ decays into $J/\psi\omega$, the experimental channel relevant to $Y(3940)$ is $\gamma p \rightarrow J/\psi\omega p$. As indicated in our calculation, the total cross section for tensor $Y(3940)$ production is much larger than that for the scalar one. In the following, with the scalar $Y(3940)$ photoproduction as an example, we discuss the background analysis relevant to $Y(3940)$ photoproduction.

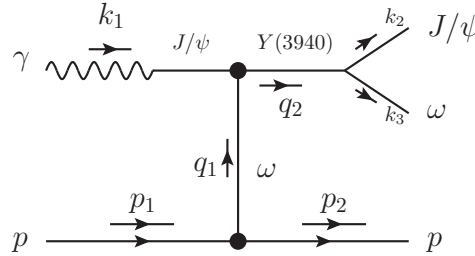


FIG. 3: The diagram depicting $\gamma p \rightarrow Y(3940)p \rightarrow J/\psi\omega p$ through ω exchange.

First we consider the $\gamma p \rightarrow J/\psi\omega p$ process as shown in Fig. 3, which corresponds to $Y(3940)$ production. The amplitude for $\gamma p \rightarrow Y(3940)p \rightarrow J/\psi\omega p$ depicted in Fig. 3 can be written as

$$\mathcal{T}_{fi} = \left[g_{\omega NN} \left(\frac{g_{Y J/\psi \omega}}{M_Y} \right)^2 \frac{e}{f_{J/\psi}} \right] \bar{u}(p_2) O^{\alpha\beta\gamma} u(p_1) \epsilon_{1\alpha} \epsilon_{2\beta} \epsilon_{3\gamma} \quad (10)$$

with

$$O^{\alpha\beta\gamma} = G^\mu \frac{\bar{g}_{\mu\nu}}{q^2 - m_\omega^2} A^{\nu\alpha\beta\gamma}, \quad G^\mu = \gamma^\mu F_{\omega NN}(q_1^2),$$

$$A^{\nu\alpha\beta\gamma} = T_{k_1, q_1}^{\alpha\nu} F_{Y J/\psi \omega}(q_1^2) \frac{1}{q_2^2 - M_Y^2 + i M_Y \Gamma} T_{k_2, k_3}^{\beta\gamma} F_{Y J/\psi \omega}(q_2^2).$$

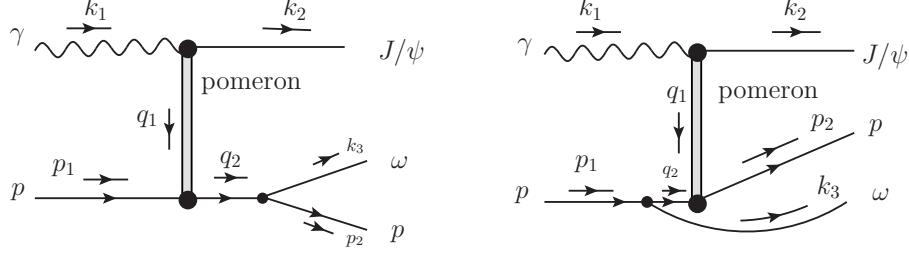


FIG. 4: The $\gamma p \rightarrow J/\psi \omega p$ process via the pomeron exchange.

Since the pomeron mediates the long-range interaction between a confined quark and a nucleon, thus $\gamma p \rightarrow J/\psi \omega p$ occurs via the pomeron exchange, which is the main background contribution to $\gamma p \rightarrow Y(3940)p \rightarrow J/\psi \omega p$. We adopt the formulas in Refs. [9, 22, 23] to describe the pomeron exchange process shown in Fig. 4.

The pomeron-nucleon coupling is determined by the vertex

$$F^\mu(t) = \frac{3\beta_0(4M_N^2 - 2.8t)}{(4M_N^2 - t)(1 - t/0.7)^2} \gamma^\mu = F(t)\gamma^\mu,$$

where $t = q_1^2$ is the exchanged pomeron momentum squared. $\beta_0^2 = 4 \text{ GeV}^2$ denotes the coupling constant between a single pomeron and a light constituent quark.

For the $\gamma V \mathcal{P}$ vertex with on-shell approximation for restoring the gauge invariance, one has

$$V_{\gamma V \mathcal{P}} = \frac{2\beta_c 4\mu_0^2}{(M_V^2 - t)(2\mu_0^2 + M_V^2 - t)} T_{\alpha\nu\beta} \epsilon_V^\beta \epsilon_\gamma^\alpha \mathcal{P}^\nu = V(t) T_{\alpha\nu\beta} \epsilon_V^\beta \epsilon_\gamma^\alpha \mathcal{P}^\nu, \quad (11)$$

$$T_{\alpha\nu\beta} = (k_\gamma + k_V)_\nu g_{\alpha\beta} - 2k_\gamma \beta g_{\nu\alpha}, \quad (12)$$

where $\beta_c^2 = 0.8 \text{ GeV}^2$ and $\mu_0 = 1.05 \text{ GeV}$.

The amplitudes for the s - and u -channel, corresponding to the diagrams on the left and on the right in Fig. 4 respectively, can be written as

$$\mathcal{T}_s^{\mathcal{P}} = G_{cc,ff} T_{\alpha\nu\beta} \bar{u}(p_2) \gamma_\xi (\not{q}_2 + m_N) \gamma^\nu u(p_1) \epsilon_\gamma^\alpha \epsilon_V^\beta \epsilon_\omega^\xi, \quad (13)$$

$$\mathcal{T}_u^{\mathcal{P}} = G_{cc,ff} T_{\alpha\nu\beta} \bar{u}(p_2) \gamma^\nu (\not{q}_2 + m_N) \gamma_\xi u(p_1) \epsilon_\gamma^\alpha \epsilon_V^\beta \epsilon_\omega^\xi \quad (14)$$

with $G_{cc,ff} = g_{\omega NN} F_{\omega NN}(q_2^2) F(t) V(t) \mathcal{G}_P(s, t) / (q_2^2 - m_N^2)$, where $\mathcal{G}_P(s, t)$ is related to the pomeron trajectory $\alpha(t) = 1 + \epsilon + \alpha' t$ via $\mathcal{G}_P(s, t) = -i(\alpha' s)^{\alpha(t)-1}$ with $\alpha' = 0.25 \text{ GeV}^{-2}$ and $\epsilon = 0.08$. $F_{\omega NN}(q_2^2) = (\Lambda_{\omega NN}^2 - m_N^2) / (\Lambda_{\omega NN}^2 - q_2^2)$.

With the transition amplitude \mathcal{T} , we obtain the total cross section of the $\gamma p \rightarrow J/\psi \omega p$ process

$$d\sigma = \frac{m_N}{2k_1 \cdot p_1} |\mathcal{T}|^2 \frac{d^3 k_2}{(2\pi)^3} \frac{1}{2k_2^0} \frac{d^3 k_3}{(2\pi)^3} \frac{1}{2k_3^0} \frac{d^3 p_2}{(2\pi)^3} \frac{m_N}{p_2^0} (2\pi)^4 \delta^4(k_1 + p_1 - k_2 - k_3 - p_2). \quad (15)$$

The numeral results are obtained by the FOWL program, which is presented in Fig. 5.

The line shape of the total cross section of $\gamma p \rightarrow J/\psi \omega p$ via ω exchange (see Fig. 5) is similar to that of $\gamma p \rightarrow Y(3940)p$ [see Fig. 2 (b)], which goes up very rapidly near the threshold and becomes flat with increasing W . The line shape of the total cross section of $\gamma p \rightarrow J/\psi \omega p$ through the pomeron exchange is monotonically increasing.

By the Dalitz plot, we can identify $Y(3940)$ by analyzing the invariant mass spectrum of $J/\psi \omega$. In Fig. 6, the Dalitz plot and the corresponding $J/\psi \omega$ invariant mass spectrum with several typical values of W are presented, where the numerical result is obtained under the upper limit of $\Gamma_{Y J/\psi \omega}$. As shown in Fig. 6, an explicit band corresponding to $Y(3940)$ appears even at the higher energy region of W , which indicates there exists a wide energy window of W to

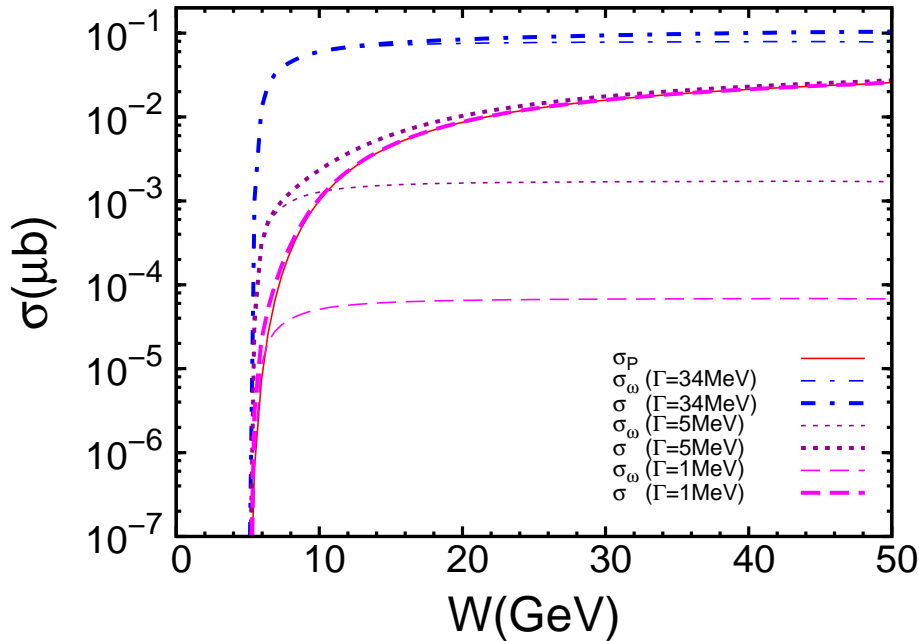


FIG. 5: The dependence of the total cross sections of $\gamma p \rightarrow J/\psi \omega p$ on $-q^2$. Here, σ_P denotes the total cross section of $\gamma p \rightarrow J/\psi \omega p$ via the pomeron exchange. σ is the total cross section of $\gamma p \rightarrow J/\psi \omega p$ via both pomeron and ω exchanges shown in Figs. 3 and 4. σ_ω means the total cross section of $\gamma p \rightarrow J/\psi \omega p$ through exchanging ω , which is related to $Y(3940)$ production directly. Since σ_ω is proportional to $g_{Y J/\psi \omega}^4$ determined by the decay width of $Y(3940) \rightarrow J/\psi$, we give the variation of σ_ω to W with several typical values of $g_{Y J/\psi \omega}$, which correspond to $\Gamma_{Y J/\psi \omega} = 1, 5, 34$ MeV.

identify $Y(3940)$ in experiments. By analyzing the invariant mass spectrum of $J/\psi \omega$, one finds that the number of events of $Y(3940)$ is up to $450/0.02\text{GeV}^2$ in 50×10^6 collisions of γp .

If a smaller decay width of $Y(3940) \rightarrow J/\psi$ is adopted, the number of events of $Y(3940)$ is reduced. We can expect that the background contribution from the pomeron exchange appears in the Dalitz plot. Here, with the numerical result corresponding to the upper limit of decay width $\Gamma_{Y J/\psi \omega}$ as an example, the Dalitz plot of $\gamma p \rightarrow J/\psi \omega p$ and the invariant mass spectrum of $J/\psi \omega$ are illustrated in Fig. 7. The number of events of $Y(3940)$ decreases to about $10/0.02\text{GeV}^2$ when taking 10^9 collisions of γp . There exists an obvious pomeron exchange contribution, a band in the bottom of the Dalitz plot. However, the bands respectively corresponding to $Y(3940)$ and the background contribution from the pomeron exchange do not interfere with each other. Thus, we still can distinguish the signal of $Y(3940)$ from the background in the Dalitz plot. We need to emphasize that the numerical results are not sensitive to the cutoffs Λ_Y/Λ_ω .

IV. CONCLUSION AND DISCUSSION

In this work, we study the possibility to search for $Y(3940)$ by the photoproduction process. Since $Y(3940)$ was observed in the invariant mass spectrum of $J/\psi \omega$, $\gamma p \rightarrow Y(3940)p$ by exchanging the ω meson is the main channel to produce $Y(3940)$. Our numerical result shows that the upper (lower) limit of the total cross section for the $\gamma p \rightarrow Y(3940)p$ is on the order of 1 nb ($0.1\text{ }\mu\text{b}$), which is comparable with the cross section of J/ψ , $\psi(2S)$ and Υ photoproduction in the HERA experiment.

Additionally we further carry out the background analysis relevant to the production of $Y(3940)$, where $\gamma p \rightarrow J/\psi \omega p$ occurs via the pomeron exchange. By the Dalitz plot, we find that the $Y(3940)$ signal can be distinguished from the background clearly. The result of the invariant mass spectrum of $J/\psi \omega$ indicates the lower limit of the number of events of $Y(3940)$ can reach up to $10/0.02\text{GeV}^2$ for 1×10^9 collisions of γp , which shows that there exists a potential to find $Y(3940)$ by meson photoproduction process. Since the calculation in this work is relevant to the decay width of $Y(3940) \rightarrow J/\psi$, to some extent we encourage our experimental colleagues to carry out the measurement of the decay width of $Y(3940) \rightarrow J/\psi$, which will be helpful to make further predictions of $Y(3940)$ production by the

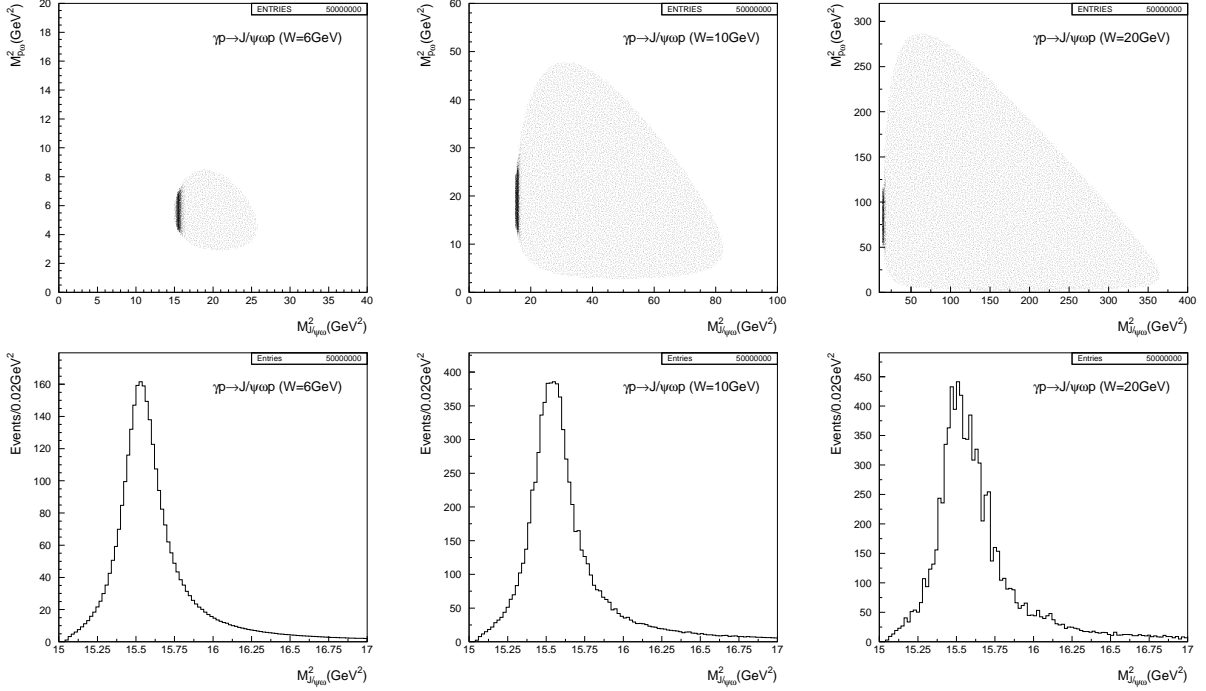


FIG. 6: The Dalitz plot (above) and the $J/\psi\omega$ invariant mass spectrum (bottom) for $\gamma p \rightarrow J/\psi\omega p$ process with the scalar $Y(3940)$ production. Here, the numerical result corresponds to the upper limit of $\Gamma_{YJ/\psi\omega}$.

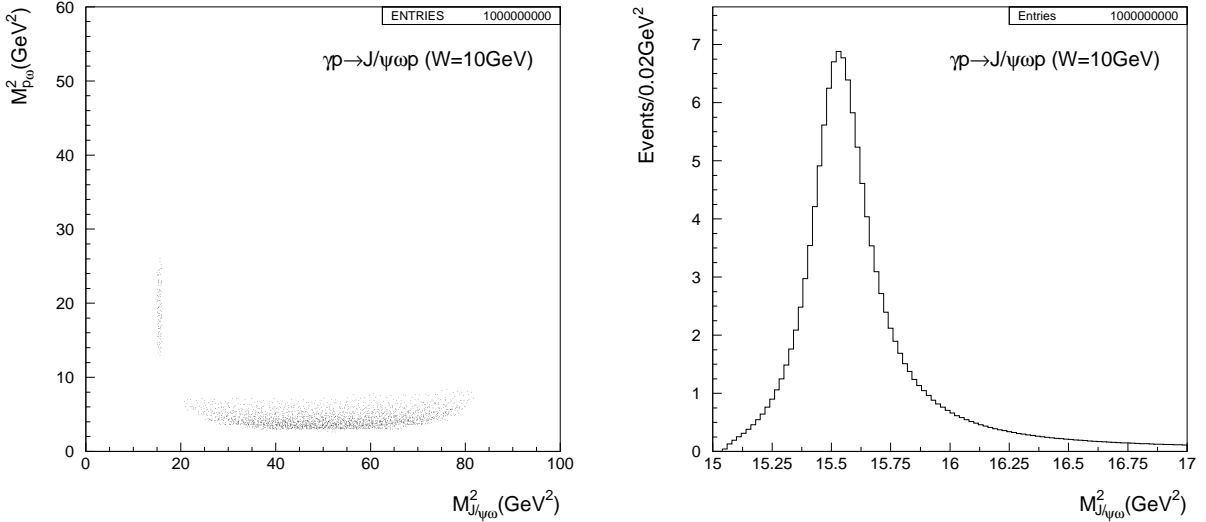


FIG. 7: The Dalitz plot (left) and the $J/\psi\omega$ invariant mass spectrum (right) for the $\gamma p \rightarrow J/\psi\omega p$ with the scalar $Y(3940)$ if taking the lower limit of $g_{YJ/\psi\omega}$ as the parameter input.

photoproduction process.

As we all know, most of the charmonium-like states X , Y , Z are observed by B meson decay. Thus, searching for these X , Y , Z states by other processes will be helpful to establish them. Besides studying the production of $Y(3940)$ and $Z(4430)$ in the meson photoproduction process, exploring the production of remaining X , Y , Z states by meson photoproduction will be an interesting topic. The experimental search for the charmonium-like states X , Y , Z is encouraged, especially for the HERA experiment.

Acknowledgements

We are grateful to Dr. Xu Cao for communication of the FOWL program. This project is supported by the National Natural Science Foundation of China under Grants No. 10705001 and No. 10905077 and the Foundation for the Author of National Excellent Doctoral Dissertation of P.R. China (FANEDD).

-
- [1] K. Abe *et al.* [Belle Collaboration], Phys. Rev. Lett. **94**, 182002 (2005) [arXiv:hep-ex/0408126].
 - [2] B. Aubert *et al.* [BaBar Collaboration], Phys. Rev. Lett. **101**, 082001 (2008) [arXiv:0711.2047 [hep-ex]].
 - [3] S. L. Zhu, Int. J. Mod. Phys. E **17**, 283 (2008) [arXiv:hep-ph/0703225].
 - [4] S. Godfrey and S. L. Olsen, Ann. Rev. Nucl. Part. Sci. **58**, 51 (2008) [arXiv:0801.3867 [hep-ph]].
 - [5] T. Aaltonen *et al.* [CDF Collaboration], Phys. Rev. Lett. **102**, 242002 (2009) [arXiv:0903.2229 [hep-ex]].
 - [6] X. Liu and S. L. Zhu, Phys. Rev. D **80**, 017502 (2009) [arXiv:0903.2529 [hep-ph]]; X. Liu and H. W. Ke, Phys. Rev. D **80**, 034009 (2009) [arXiv:0907.1349 [hep-ph]]; X. Liu, Phys. Lett. B **680**, 137 (2009) [arXiv:0904.0136 [hep-ph]].
 - [7] T. Branz, T. Gutsche and V. E. Lyubovitskij, arXiv:0903.5424 [hep-ph].
 - [8] S. K. Choi *et al.* [BELLE Collaboration], Phys. Rev. Lett. **100**, 142001 (2008) [arXiv:0708.1790 [hep-ex]].
 - [9] X. H. Liu, Q. Zhao and F. E. Close, Phys. Rev. D **77**, 094005 (2008) [arXiv:0802.2648 [hep-ph]].
 - [10] H. W. Ke and X. Liu, Eur. Phys. J. C **58**, 217 (2008) [arXiv:0806.0998 [hep-ph]].
 - [11] S. Chekanov *et al.* [ZEUS Collaboration], Eur. Phys. J. C **24**, 345 (2002) [arXiv:hep-ex/0201043].
 - [12] S. Chekanov *et al.* [ZEUS Collaboration], Eur. Phys. J. C **27**, 173 (2003) [arXiv:hep-ex/0211011].
 - [13] S. Chekanov *et al.* [ZEUS Collaboration], Nucl. Phys. B **695**, 3 (2004) [arXiv:hep-ex/0404008].
 - [14] D. Black, M. Harada and J. Schechter, Phys. Rev. Lett. **88**, 181603 (2002) [arXiv:hep-ph/0202069].
 - [15] Y. s. Oh and T. S. H. Lee, Phys. Rev. C **69**, 025201 (2004) [arXiv:nucl-th/0306033].
 - [16] B. Renner, Nucl. Phys. B **30**, 634 (1971).
 - [17] J. P. Lansberg and T. N. Pham, Phys. Rev. D **79**, 094016 (2009) [arXiv:0903.1562 [hep-ph]].
 - [18] C. Amsler *et al.* [Particle Data Group], Phys. Lett. B **667**, 1 (2008).
 - [19] A. M. Gasparyan, J. Haidenbauer, C. Hanhart and J. Speth, Phys. Rev. C **68**, 045207 (2003) [arXiv:nucl-th/0307072].
 - [20] S. Chekanov *et al.* [ZEUS Collaboration], arXiv:0903.4205 [hep-ex].
 - [21] J. Breitweg *et al.* [ZEUS Collaboration], Phys. Lett. B **437**, 432 (1998) [arXiv:hep-ex/9807020].
 - [22] A. Donnachie and P. V. Landshoff, Phys. Lett. B **185**, 403 (1987).
 - [23] M. A. Pichowsky and T. S. H. Lee, Phys. Lett. B **379**, 1 (1996) [arXiv:nucl-th/9601032].